



---

## Figures and figure supplements

Conversion of random X-inactivation to imprinted X-inactivation by maternal PRC2

**Clair Harris et al**

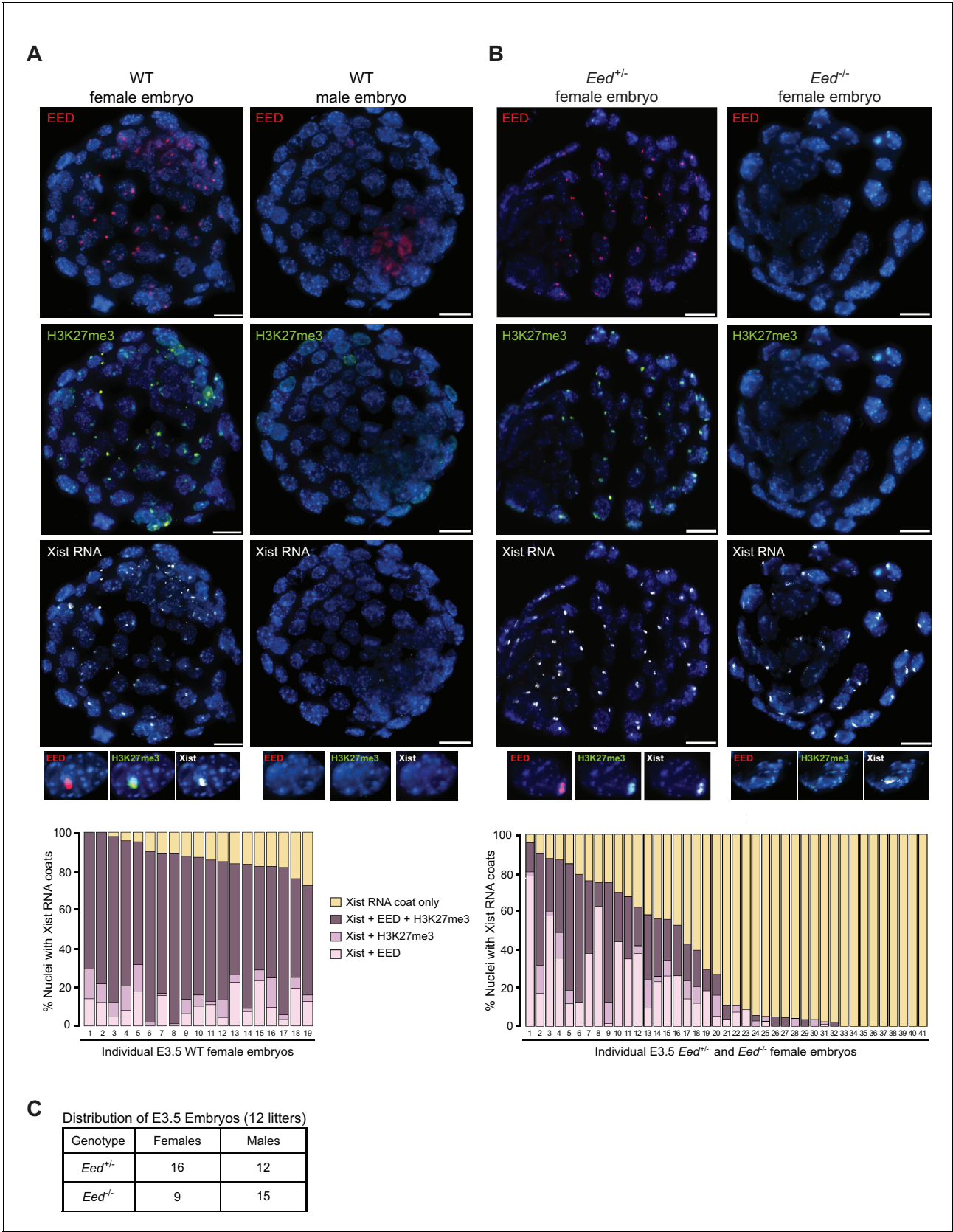


**Figure 1.** Coincident accumulation of EED and H3K27me3 on the inactive X-chromosome in blastocyst-stage WT, *Eed*<sup>+/-</sup> and *Eed*<sup>-/-</sup> mouse embryos. See also **Figure 1—figure supplement 1**. (A,B) RNA FISH detection of Xist RNA (white) and immunofluorescence (IF) detection of EED (red) and H3K27me3 (green). *Figure 1 continued on next page*

## Figure 1 continued

H3K27me3 (green) in representative female and male wild-type (WT) (A) or female *Eed*<sup>+/-</sup> and *Eed*<sup>-/-</sup> (B) E3.0 – E3.5 blastocyst embryos. Nuclei are stained blue with DAPI. Scale bars, 20  $\mu$ m. Embryos ranged in size from 23 to 57 nuclei. Bar plots, percentage of nuclei with coincident accumulation of Xist RNA and EED and/or H3K27me3 enrichment in individual embryos. (C) Genotype and sex distribution of *Eed*<sup>+/-</sup> and *Eed*<sup>-/-</sup> mouse blastocyst embryos from the cross in (B). The difference between the frequency of *Eed*<sup>+/-</sup> vs *Eed*<sup>-/-</sup> male and female embryos is not significant ( $p>0.05$ , Two-tailed Student's T-test).

DOI: <https://doi.org/10.7554/eLife.44258.003>

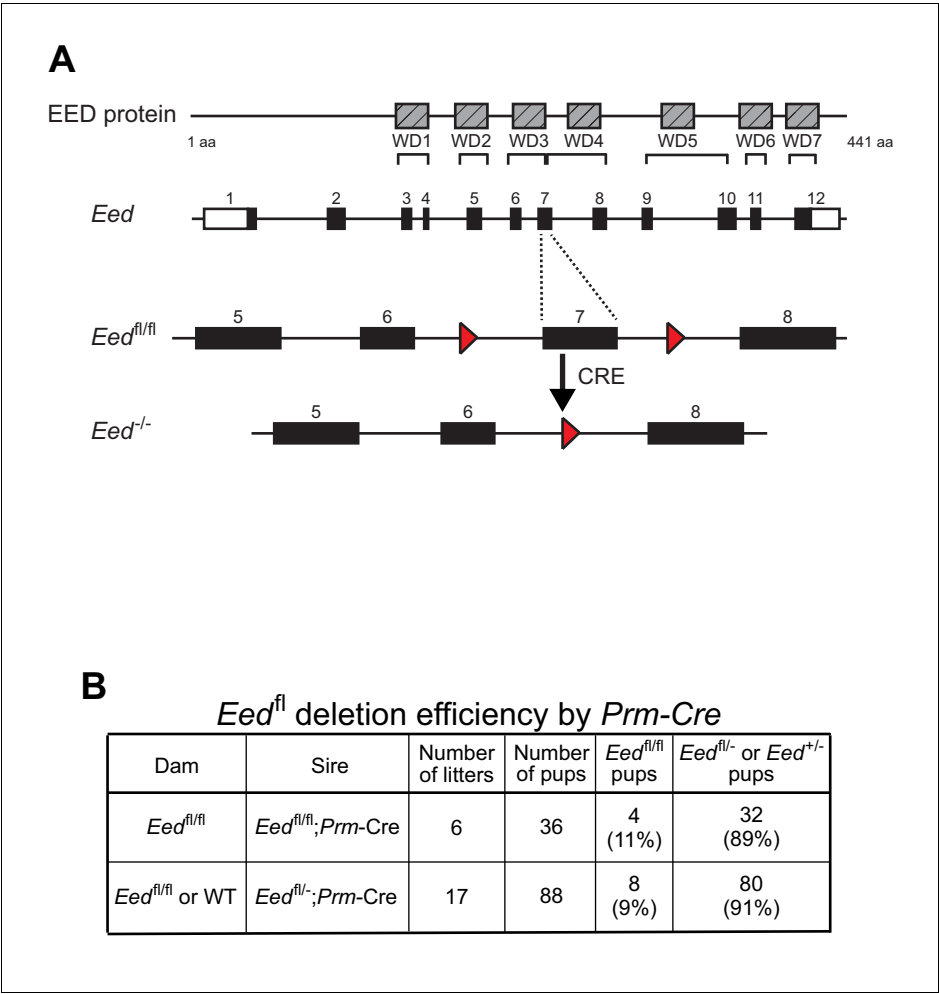


**Figure 1—figure supplement 1.** Generation of *Eed*<sup>-/-</sup> embryos. (A) Schematic depicting the deletion of floxed *Eed* exon seven by CRE recombinase. (B) Breeding data showing the efficiency of *Prm-Cre* deletion of the *Eed*<sup>fl</sup> allele.

DOI: <https://doi.org/10.7554/eLife.44258.004>



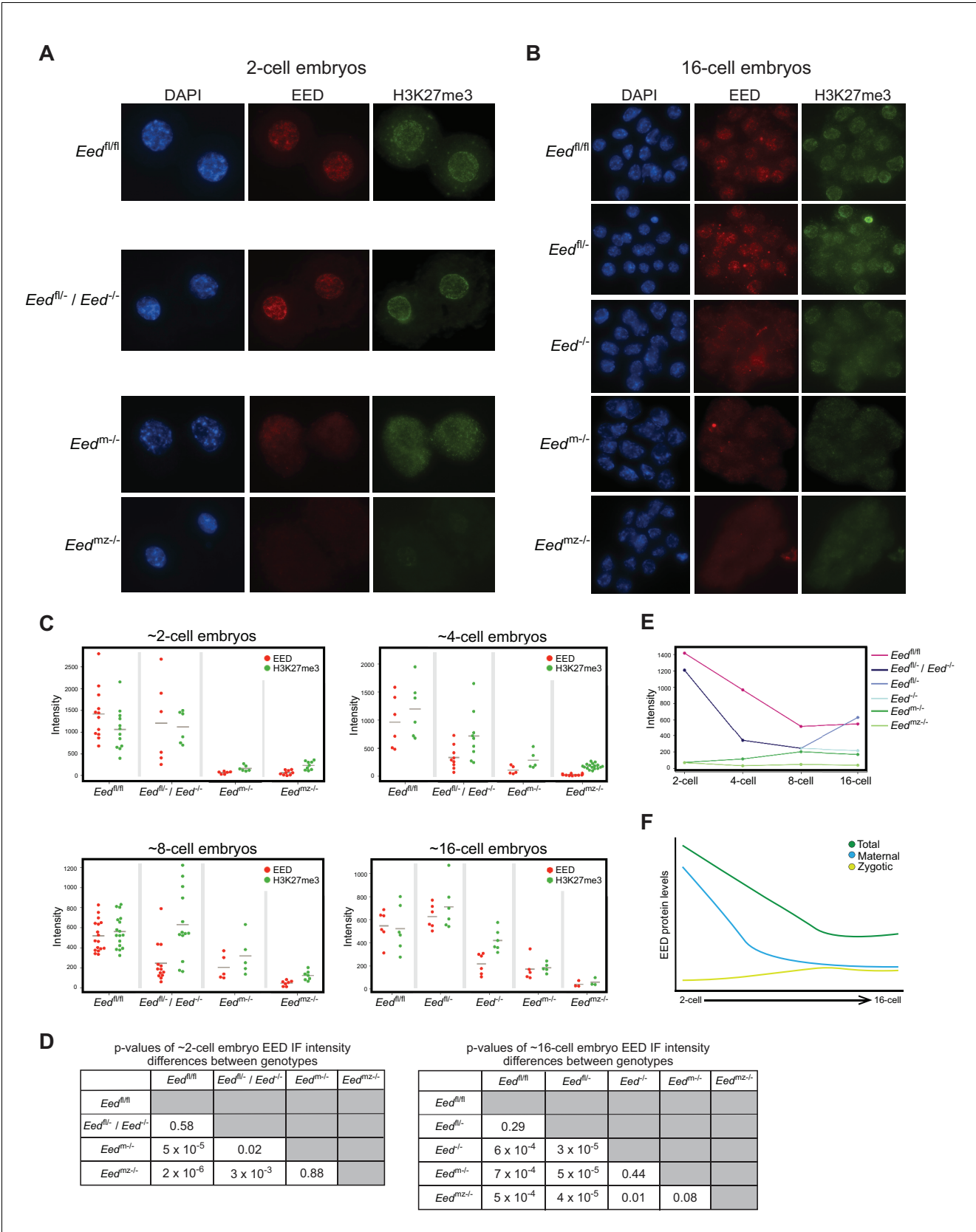


**Figure 2.** Assessment of maternal and zygotic EED expression in early preimplantation embryos. See also **Figure 2—figure supplement 1**, and **Figure 2—source data 1**. (A,B) Immunofluorescent (IF) detection of EED (red) and H3K27me3 (green) in 2- and 16-cell *Eed<sup>fl/fl</sup>*, *Eed<sup>fl/-</sup> / Eed<sup>+/-</sup>*, *Eed<sup>m/-</sup>*, *Eed<sup>mz/-</sup>*. Figure 2 continued on next page

## Figure 2 continued

and *Eed*<sup>mz/-</sup> embryos. Nuclei are stained blue by DAPI. (C) Dot plots of EED and H3K27me3 IF signals in the five genotypes (*Eed*<sup>fl/fl</sup>, *Eed*<sup>fl/-</sup>, *Eed*<sup>-/-</sup>, *Eed*<sup>m/-</sup>, *Eed*<sup>mz/-</sup>) at the ~2-cell, ~4-cell, ~8-cell, and ~16-cell stage. Each dot represents an individual embryo. The gray line indicates mean fluorescence intensity. Pairwise statistical comparisons between all genotypes are included in **Supplementary file 1**. (D) Significance testing of differences in EED fluorescence intensity in ~2-cell embryos and ~16-cell embryos plotted in (C) (Two-tailed Student's T-test). (E) Mean EED fluorescence intensity from data in (C) plotted across early embryogenesis. (F) Model of change in maternal, zygotic, and total EED expression levels during early embryonic development.

DOI: <https://doi.org/10.7554/eLife.44258.005>

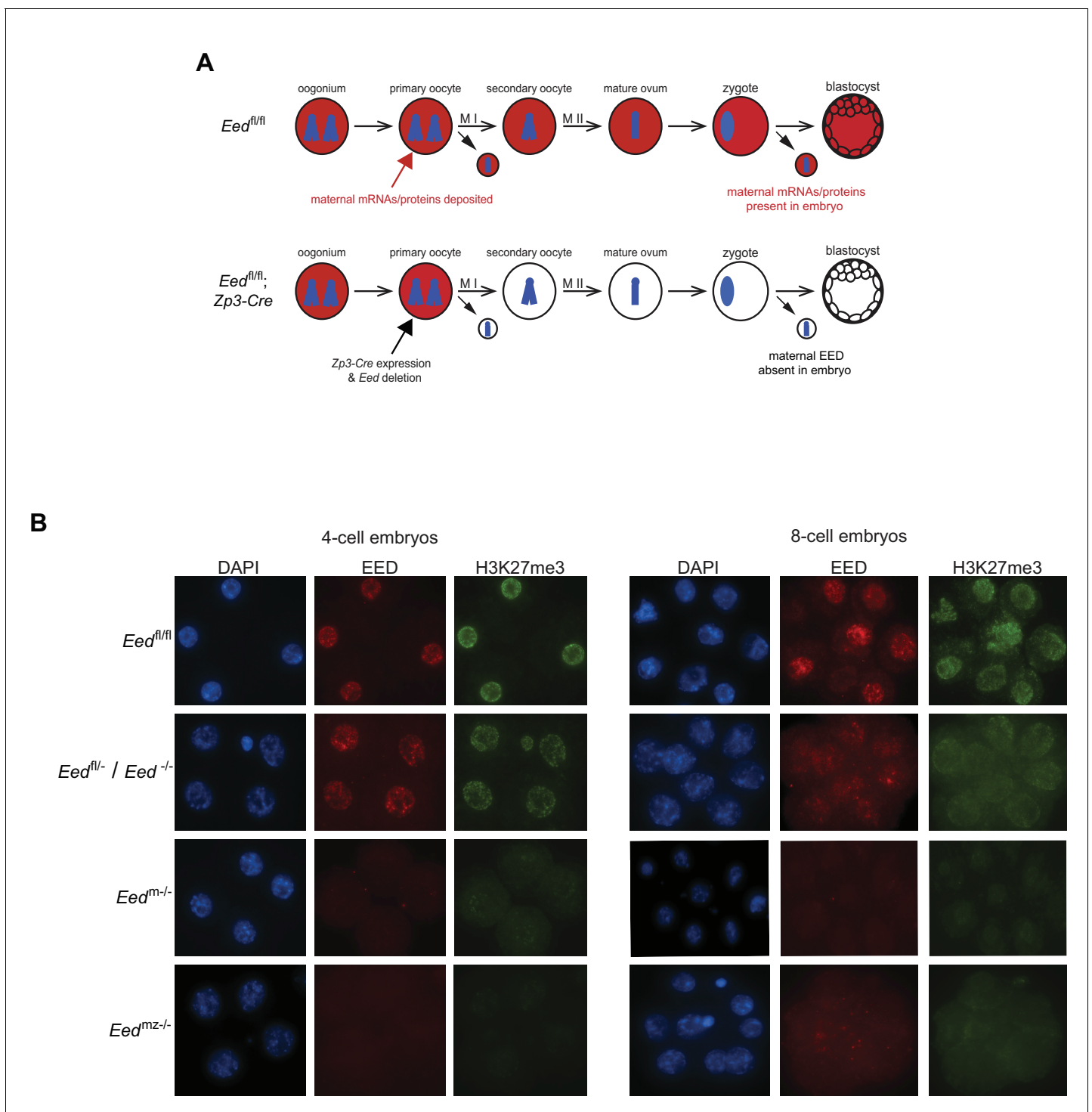


**Figure 2—figure supplement 1.** Analysis of EED and H3K27me3 fluorescence intensity in *Eed* mutants. (A) Schematic depicting the deletion of *Eed* exon seven by *Zp3-Cre* used to generate embryos maternally null for *Eed*. (B) Representative images of *Eed<sup>fl/fl</sup>*, *Eed<sup>fl/-</sup>*, *Eed<sup>-/-</sup>*, *Eed<sup>m/-</sup>*, and *Eed<sup>mz/-</sup>* 4- and 8-cell embryos stained by IF for EED and H3K27me3. Nuclei are indicated by blue DAPI stain, EED stain is indicated in red, and H3K27me3 stain is indicated in green.

DOI: <https://doi.org/10.7554/eLife.44258.006>

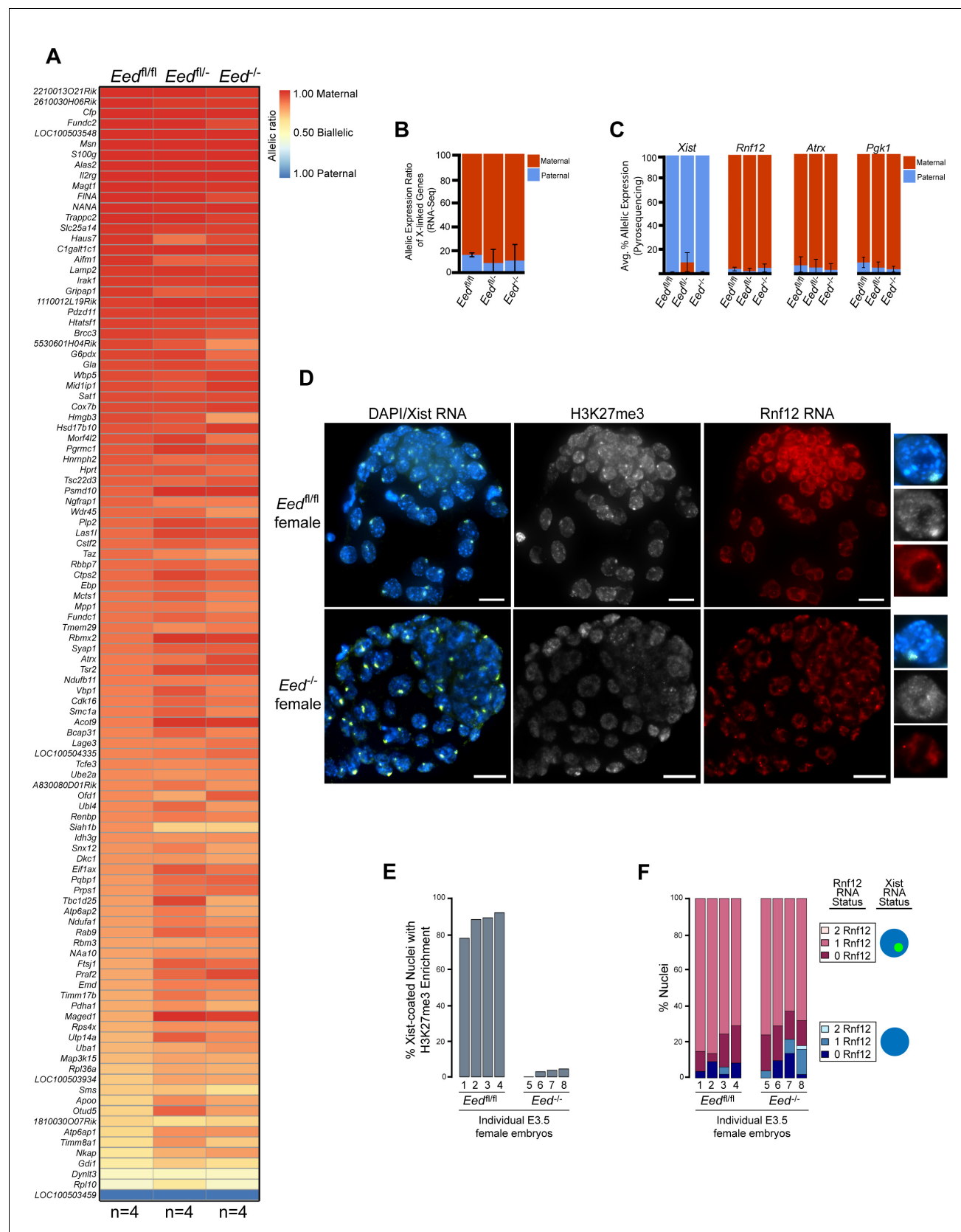


**Figure 3.** Lack of defective X-inactivation initiation in *Eed*<sup>-/-</sup> blastocysts. See also **Figure 3—figure supplement 1**. (A) Allele-specific X-linked gene expression heat map of female *Eed*<sup>fl/fl</sup>, *Eed*<sup>fl/+</sup>, and *Eed*<sup>-/-</sup> blastocysts. Four embryos each of *Eed*<sup>fl/fl</sup>, *Eed*<sup>fl/+</sup>, and *Eed*<sup>-/-</sup> genotypes were sequenced. Figure 3 continued on next page

## Figure 3 continued

individually and only genes with informative allelic expression in all samples are plotted (see Materials and methods). Genes are ordered on the basis of allelic expression in *Eed<sup>fl/fl</sup>* embryos. (B) Average allelic expression of the RNA-Seq data shown in (A). The mean allelic expression of X-linked genes lacks significant difference between each combination of the three genotypes ( $p > 0.05$ , Welch's two-sample T-test). Pairwise statistical comparisons between all genotypes are included in **Supplementary file 3**. (C) Pyrosequencing-based quantification of allelic expression of X-linked genes *Xist*, *Rnf12*, *Atrx* and *Pgk1* in *Eed<sup>fl/fl</sup>*, *Eed<sup>fl/-</sup>*, and *Eed<sup>-/-</sup>* blastocysts. Error bars represent the standard deviation of data from 3 to 6 independent blastocyst embryos. The mean allelic expression of all four genes lack significant difference between each combination of the three genotypes ( $p > 0.05$ , Welch's two-sample T-test). Pairwise statistical comparisons for all genes and between all genotypes are included in **Supplementary file 4**. (D) RNA FISH detection of *Xist* RNA (green), *Rnf12* RNA (red), and IF detection of H3K27me3 (white) in representative *Eed<sup>fl/fl</sup>* or *Eed<sup>-/-</sup>* female blastocysts. Nuclei are stained blue with DAPI. Scale bars, 20  $\mu$ m. Individual nuclei displaying representative categories of stains are shown to the right of each embryo. Embryos ranged in size from 39 to 100 nuclei. (E) Bar plot of percentage of nuclei with coincident accumulation of *Xist* RNA and H3K27me3 in individual *Eed<sup>fl/fl</sup>* and *Eed<sup>-/-</sup>* embryos. Each bar is an individual embryo. Embryo numbers under the bars correspond to the same embryos plotted in (F). (F) Bar plots of percentage of nuclei with or without *Xist* RNA-coating and *Rnf12* RNA expression in the embryos stained in (D) and plotted in (E). The numbers under the bars correspond to the same embryos plotted in (E).

DOI: <https://doi.org/10.7554/eLife.44258.008>

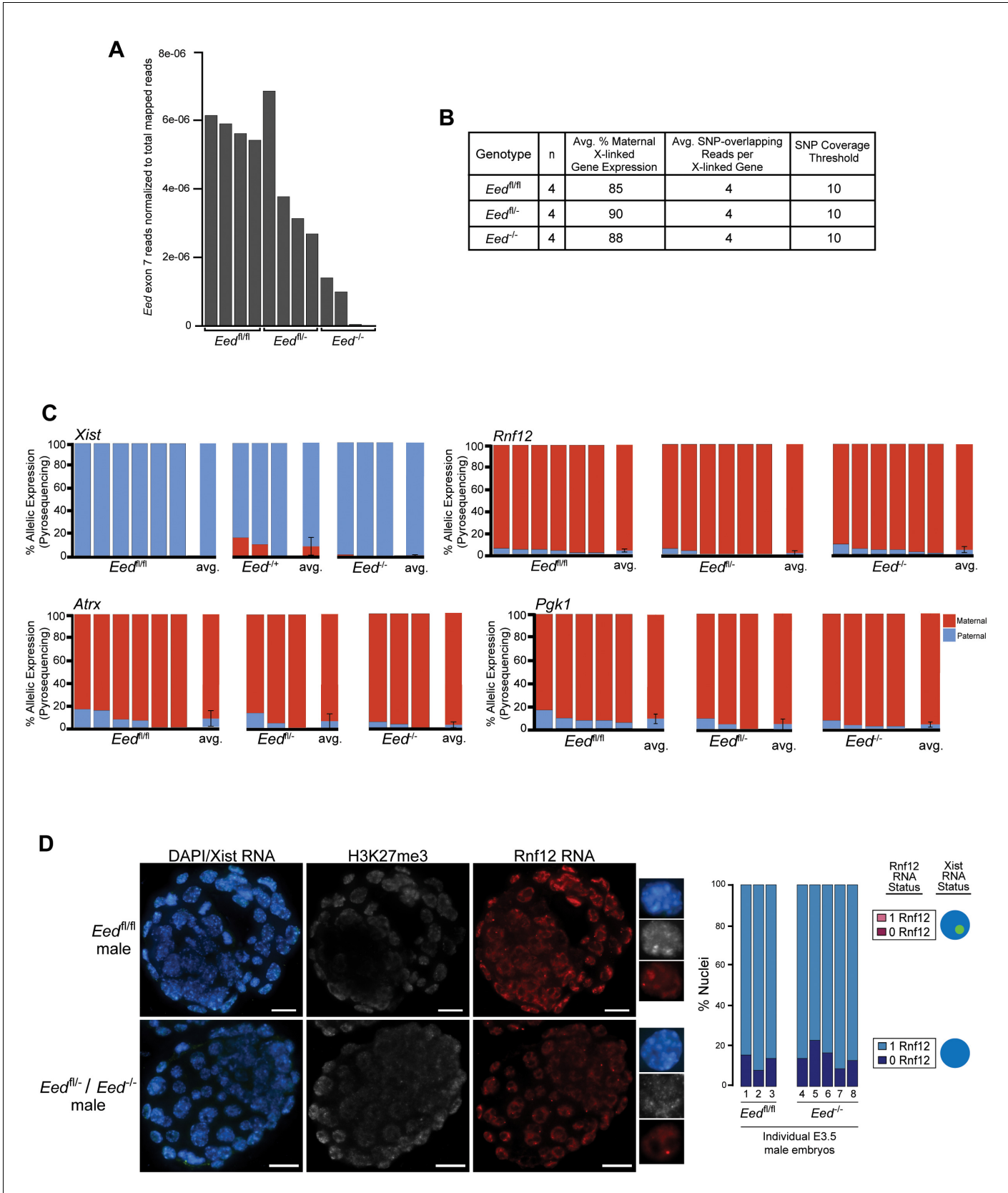


## Figure 3—figure supplement 1 continued

number of sequenced embryos, average % maternal X-linked gene expression, average number of SNPs per X-linked gene, and the SNP overlapping read coverage threshold. A comprehensive list of expression levels of all informative genes is included in **Supplementary file 2**. (C) Pyrosequencing-based quantification of allelic expression of X-linked genes *Xist*, *Rnf12*, *Atrx*, and *Pgk1* in individual *Eed<sup>fl/fl</sup>*, *Eed<sup>fl/-</sup>*, and *Eed<sup>-/-</sup>* female blastocysts. Error bars, standard deviation of data from 3 to 6 independent embryos. The mean allelic expression of all four genes lacks significant difference between each combination of the three genotypes ( $p > 0.05$ , Welch's two-sample T-test). Pairwise statistical comparisons for all genes and between all genotypes are included in **Supplementary file 4**. (D) RNA FISH detection of *Xist* RNA (green), *Rnf12* RNA (red), and IF detection of H3K27me3 (white) in representative *Eed<sup>fl/fl</sup>* and *Eed<sup>fl/-</sup>* or *Eed<sup>-/-</sup>* male blastocysts. Nuclei are stained blue with DAPI. Scale bars, 20  $\mu\text{m}$ . Right of each embryo, individual nuclei displaying representative categories of stains. Embryos ranged in size from 56 to 65 nuclei. Bar plot, percentage of nuclei with or without *Xist* RNA-coating and *Rnf12* RNA expression.

DOI: <https://doi.org/10.7554/eLife.44258.009>



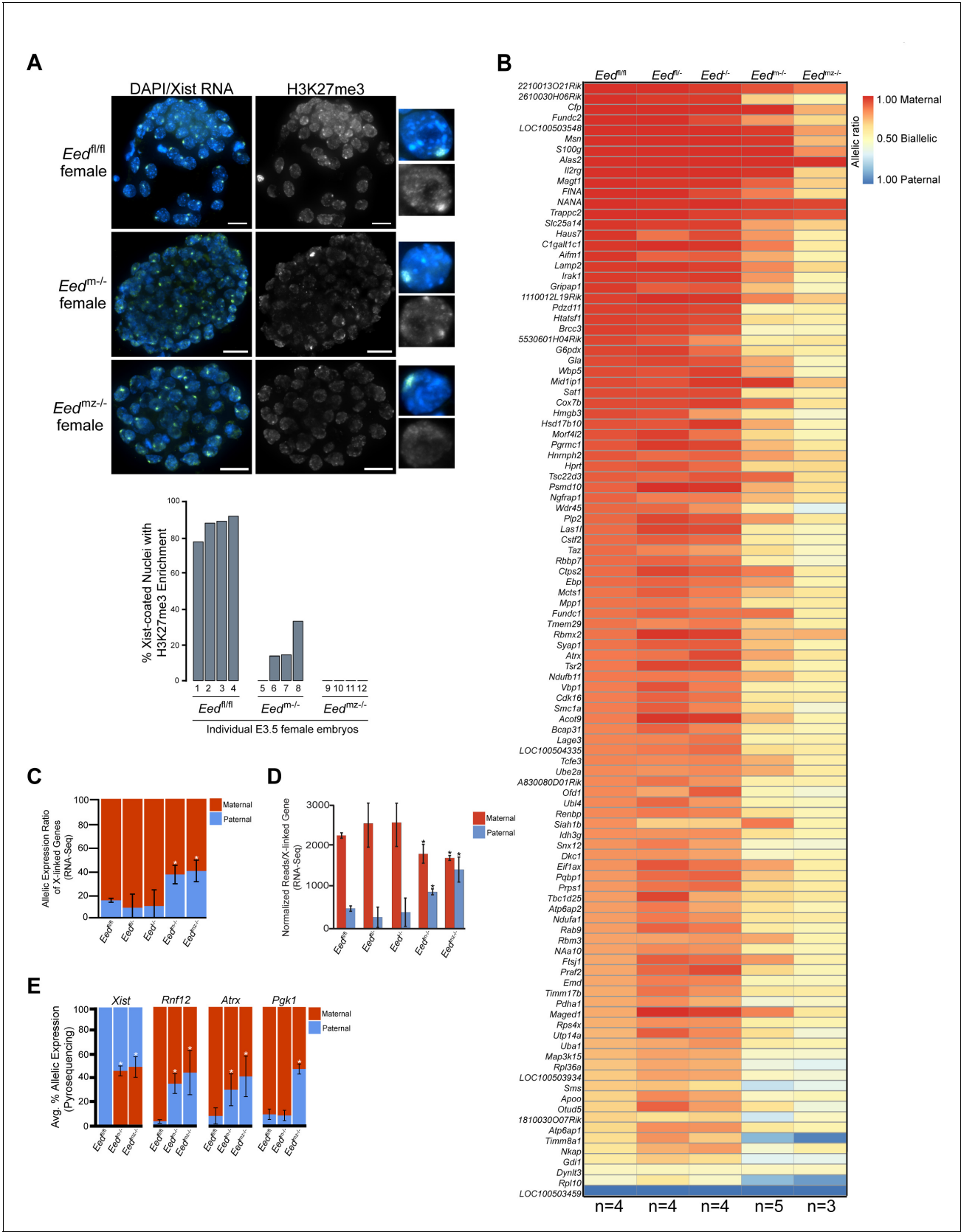


**Figure 4.** Defective imprinted X-inactivation initiation in blastocysts lacking maternal EED. See also **Figure 4—figure supplement 1**. (A) RNA FISH detection of Xist RNA (green) and IF stain for H3K27me3 (white) in representative *Eed<sup>m/-</sup>* and *Eed<sup>mz/-</sup>* female blastocysts. Nuclei are stained blue with DAPI. (B) Heatmap of allelic expression ratios for 100 genes in EED-deficient blastocysts. (C) Bar graph of allelic expression ratios for X-linked genes. (D) Bar graph of normalized reads for X-linked genes. (E) Bar graph of average allelic expression for X-linked genes. *Figure 4 continued on next page*



## Figure 4 continued

DAPI. Scale bars, 20  $\mu\text{m}$ . *Eed<sup>fl/fl</sup>* blastocyst from **Figure 3D** shown for comparison. Right, individual representative nuclei. Mutant embryos ranged in size from 46 to 80 nuclei. Bar plot shows percentage of nuclei in each embryo analyzed that displayed H3K27me3 enrichment on the Xist RNA-coated X-chromosome. **(B)** Maternal:paternal X-linked gene expression heat map of female *Eed<sup>m-/-</sup>* and *Eed<sup>mz-/-</sup>* blastocysts. Five *Eed<sup>m-/-</sup>* and three *Eed<sup>mz-/-</sup>* embryos were sequenced individually and only genes with informative allelic expression in all samples are plotted (see Materials and methods). *Eed<sup>fl/fl</sup>*, *Eed<sup>fl/-</sup>*, and *Eed<sup>l/-</sup>* data from **Figure 3A** shown for comparison. Genes are ordered on the basis of allelic expression in *Eed<sup>fl/fl</sup>* embryos. **(C)** Average maternal:paternal X-linked gene expression ratio from the RNA-Seq data shown in **B**. *Eed<sup>fl/fl</sup>*, *Eed<sup>fl/-</sup>*, and *Eed<sup>l/-</sup>* data from **Figure 3B** shown for comparison. The mean allelic expression of X-linked genes is significantly different between *Eed<sup>m-/-</sup>* and *Eed<sup>fl/fl</sup>*, and *Eed<sup>mz-/-</sup>* and *Eed<sup>fl/fl</sup>* blastocysts. ( $p < 0.05$ , Welch's two-sample T-test). Pairwise statistical comparisons between all genotype groups are included in **Supplementary file 3**. **(D)** Average normalized maternal and paternal X-linked gene expression in blastocysts. Maternal and paternal X-linked gene expression is significantly different between *Eed<sup>m-/-</sup>* and *Eed<sup>mz-/-</sup>* embryos compared to *Eed<sup>fl/fl</sup>* embryos (\*,  $p < 0.05$ , Two-tailed Student's T-test). Pairwise statistical comparisons between all genotypes are included in **Supplementary file 3**. **(E)** Pyrosequencing-based quantification of allelic expression of X-linked genes in *Eed<sup>m-/-</sup>* and *Eed<sup>mz-/-</sup>* blastocysts. *Eed<sup>fl/fl</sup>* data from **Figure 3C** are shown for comparison. Error bars represent the standard deviation of data from 3 to 6 independent blastocyst embryos. The mean allelic expression of *Xist*, *Rnf12*, and *Atrx* is significantly different between *Eed<sup>fl/fl</sup>* and *Eed<sup>m-/-</sup>* embryos. The mean allelic expression of *Xist*, *Rnf12*, *Pgk1*, and *Atrx* is significantly different between *Eed<sup>fl/fl</sup>* and *Eed<sup>mz-/-</sup>* embryos ( $p < 0.05$ , Welch's two-sample T-test). Pairwise statistical comparisons for all genes and between all genotypes are included in **Supplementary file 4**.

DOI: <https://doi.org/10.7554/eLife.44258.010>

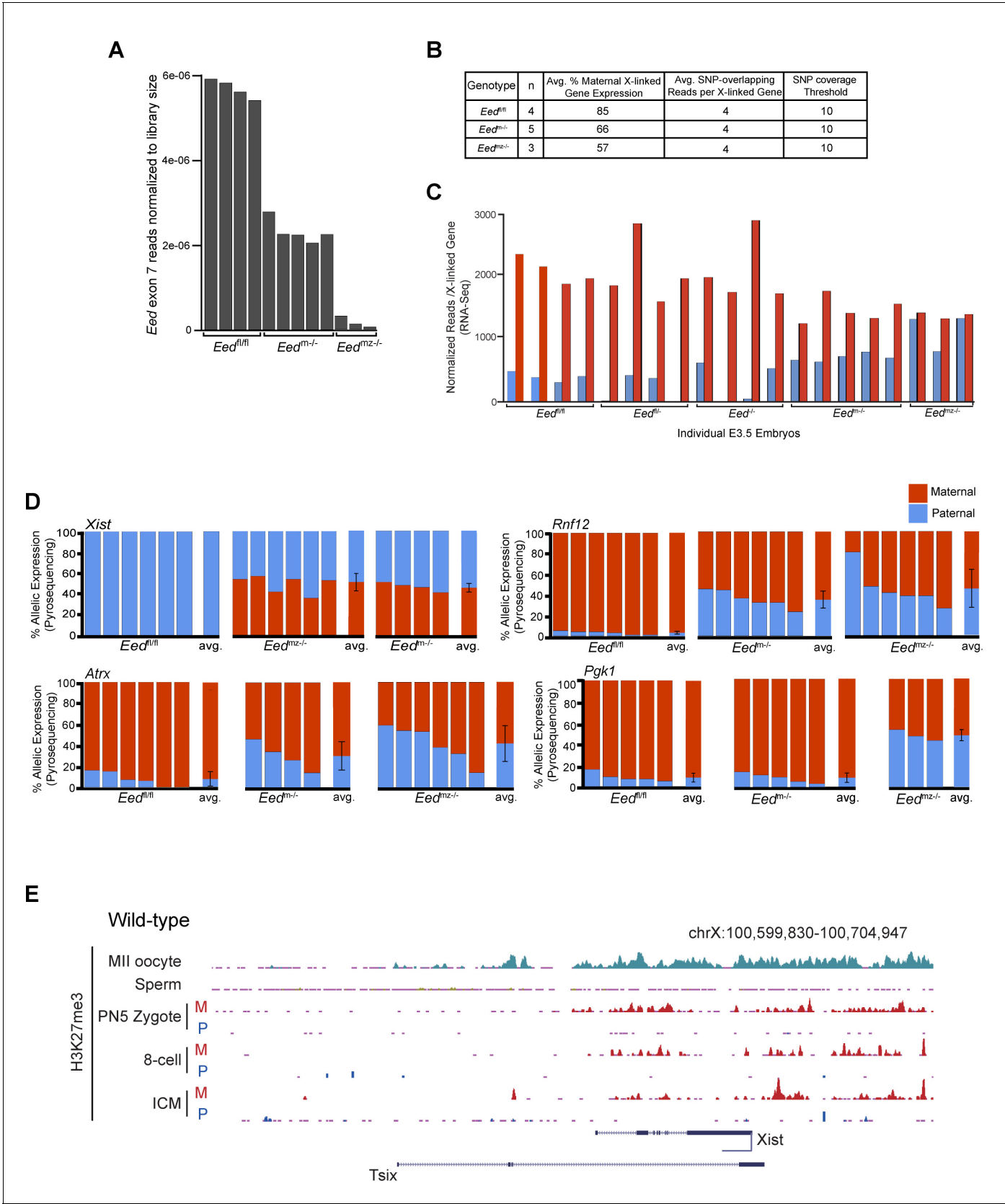


**Figure 4—figure supplement 1.** Generation and X-linked gene profiling of *Eed<sup>m-/+</sup>* and *Eed<sup>m2-/-</sup>* embryos. (A) Validation of genotypes of E3.5 female embryos. *Eed* exon 7 RNA-Seq reads are normalized to total mapped RNA-Seq reads. (B) Table describing the RNA-Seq genotypes, number of Figure 4—figure supplement 1 continued on next page

## Figure 4—figure supplement 1 continued

sequenced embryos, average percentage maternal X-linked gene expression, average number of SNPs per X-linked gene, and the SNP overlapping read coverage threshold. A comprehensive list of expression levels of all informative genes is included in **Supplementary file 2**. (C) Normalized maternal or paternal reads per X-linked gene in individual  $Eed^{fl/fl}$ ,  $Eed^{fl/-}$ ,  $Eed^{-/-}$ ,  $Eed^{mz/-}$ , and  $Eed^{mz/-}$  female E3.5 blastocysts. (D) Pyrosequencing-based quantification of allelic expression of X-linked genes *Xist*, *Rnf12*, *Atrx*, and *Pgk1* in individual  $Eed^{fl/fl}$ ,  $Eed^{mz/-}$ , and  $Eed^{mz/-}$  female E3.5 blastocysts. Error bars, standard deviation of data from 3 to 6 independent embryos. The mean allelic expression for *Xist*, *Rnf12*, and *Atrx* is significantly different between  $Eed^{fl/fl}$  and  $Eed^{mz/-}$  embryos ( $p < 0.05$ , Welch's two-sample T-test). The mean allelic expression for *Xist*, *Rnf12*, *Atrx*, and *Pgk1* is significantly different between  $Eed^{fl/fl}$  and  $Eed^{mz/-}$  embryos ( $p < 0.05$ , Welch's two-sample T-test). The mean allelic expression of *Pgk1* is significantly different between  $Eed^{mz/-}$  and  $Eed^{mz/-}$  embryos ( $p < 0.05$ , Welch's two-sample T-test). Pairwise statistical comparisons for all genes and between all genotypes are included in **Supplementary file 4**. (E) Allele-specific H3K27me3 ChIP-Seq at the *Xist* locus of wild-type MII oocyte, sperm, PN5 zygote, 8 cell embryo, and inner cell mass (ICM) (Zheng et al., 2016).

DOI: <https://doi.org/10.7554/eLife.44258.011>

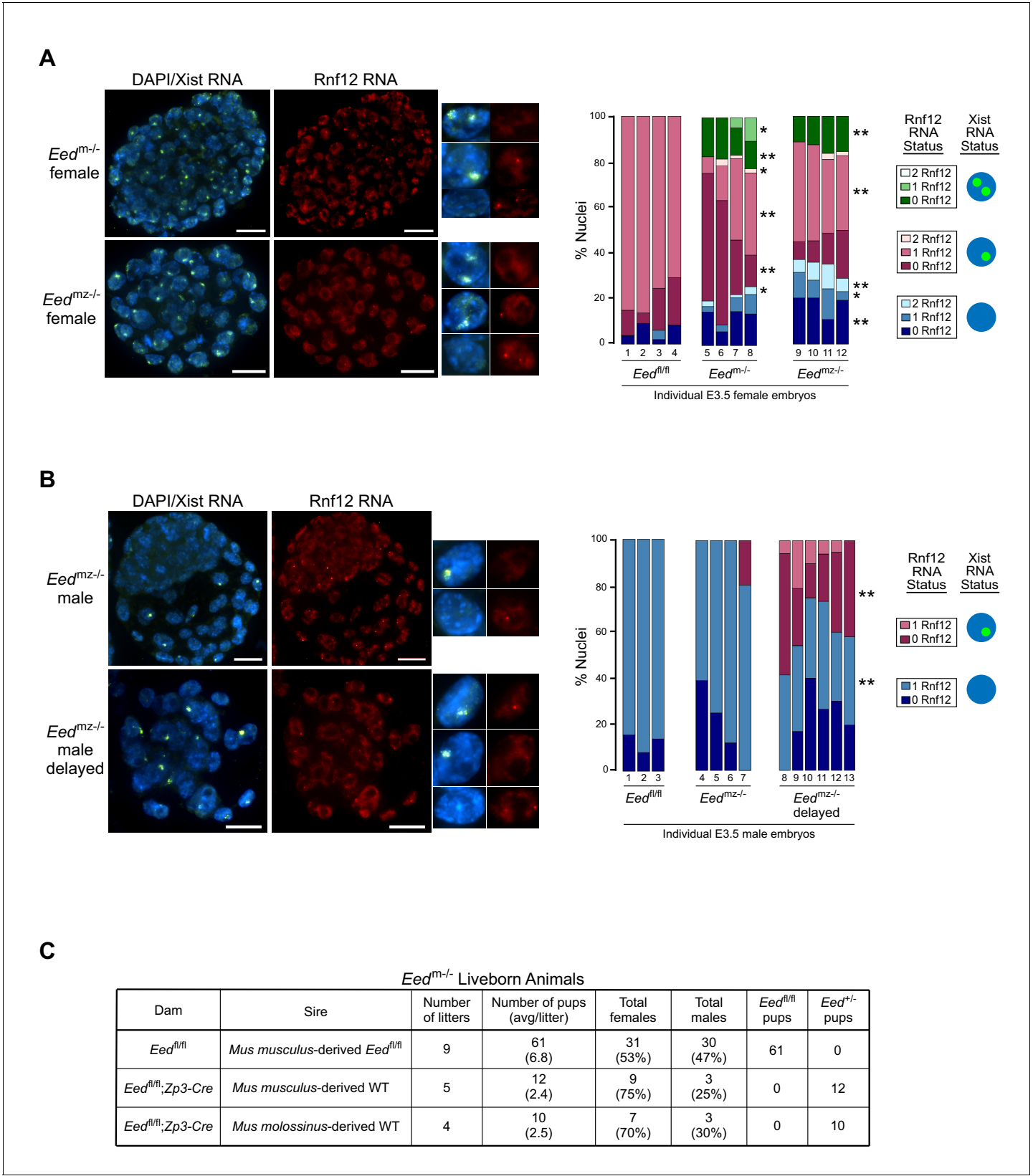


**Figure 5.** RNA FISH analysis of X-inactivation in *Eed<sup>m/-</sup>* and *Eed<sup>mz/-</sup>* blastocysts. (A,B) RNA FISH detection of Xist RNA (green) and Rnf12 RNA (red) in representative *Eed<sup>m/-</sup>* and *Eed<sup>mz/-</sup>* female (A) and *Eed<sup>mz/-</sup>* male (B) blastocysts. Nuclei are stained blue with DAPI. Scale bars, 20  $\mu$ m. Individual nuclei of representative categories of stain are shown to the right of each embryo. *Eed<sup>fl/fl</sup>* female data from **Figure 3D** shown for comparison. Mutant female **Figure 5 continued on next page**

## Figure 5 continued

embryos ranged in size from 46 to 80 nuclei. Fully developed mutant male embryos ranged in size from 53 to 110 nuclei. Delayed mutant male embryos ranged in size from 30 to 40 nuclei. Bar plot shows percentage of nuclei in each embryo with Xist RNA coats and/or Rnf12 RNA expression. Each bar represents an individual embryo and embryo numbers under the bars correspond to the same female embryos plotted in **Figure 4A**. \*,  $p < 0.05$ ; \*\*,  $p < 0.01$ , Two-tailed Student's T-test, between  $Eed^{m/-}$  and  $Eed^{fl/fl}$ , or  $Eed^{mz/-}$  and  $Eed^{fl/fl}$ . (C) Data showing the number of  $Eed^{m/-}$  embryos which can live to term compared to  $Eed^{fl/fl}$  embryos. WT, wild-type. Table shows  $Eed^{m/-}$  litters sired by *Mus musculus*-derived male or *Mus molossinus*-derived male. Male  $Eed^{m/-}$  offspring are underrepresented compared to females,  $p = 0.02$ , Two-tailed Student's T-test.

DOI: <https://doi.org/10.7554/eLife.44258.012>

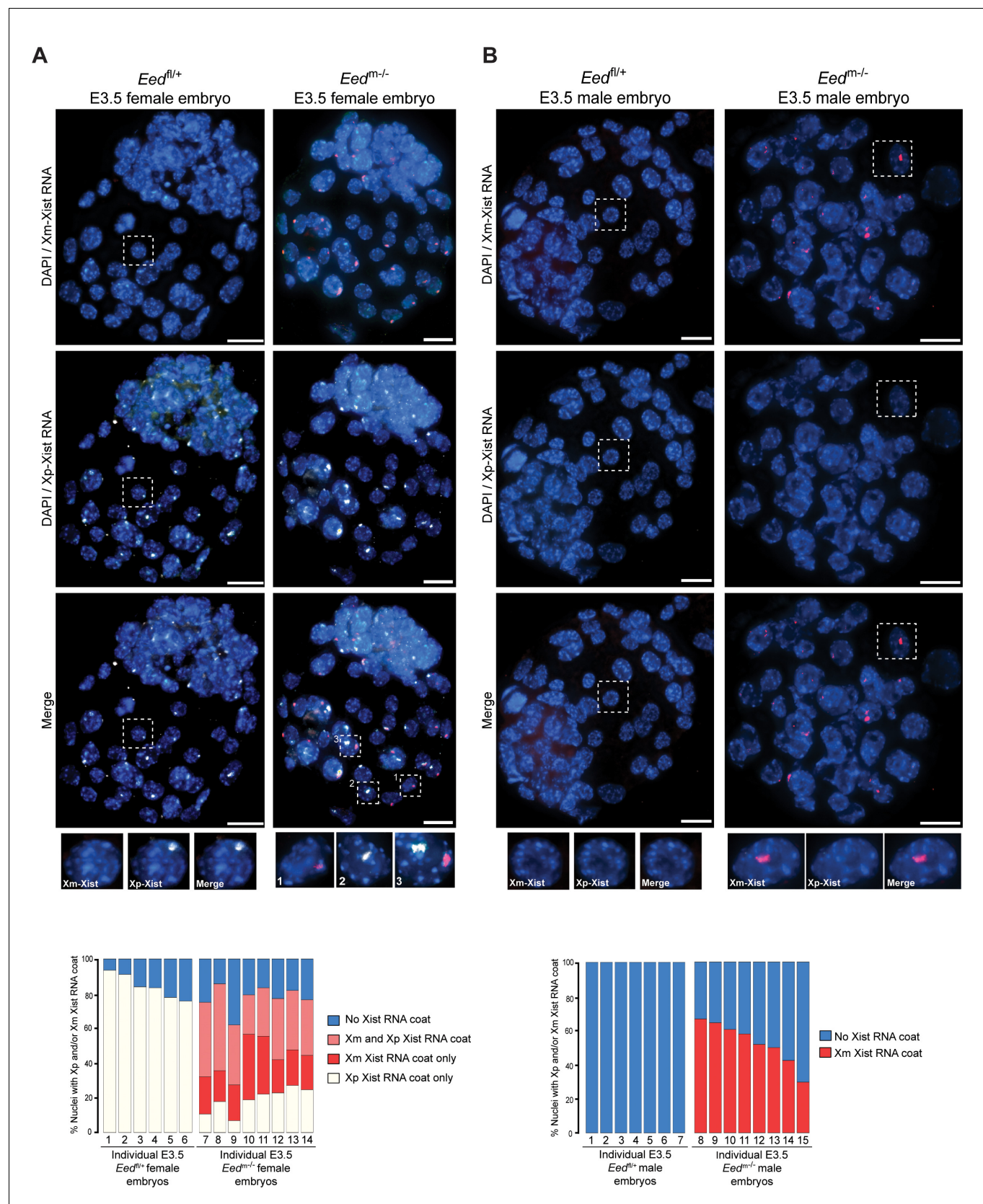


**Figure 6.** Switching of imprinted to random X-inactivation in E3.5 embryos lacking maternal EED. See also **Figure 6—figure supplement 1**. (A,B) Allele-Specific Xist RNA FISH in *Eed<sup>fl/+</sup>* and *Eed<sup>m/-</sup>* male and female E3.0-E3.5 blastocyst embryos. Xist RNA expressed from the maternal X-

Figure 6 continued on next page

*Figure 6 continued*

chromosome is indicated in red and from the paternal X-chromosome in white. Representative embryos are depicted. Nuclei are stained blue with DAPI. Scale bars, 20  $\mu\text{m}$ .

DOI: <https://doi.org/10.7554/eLife.44258.013>



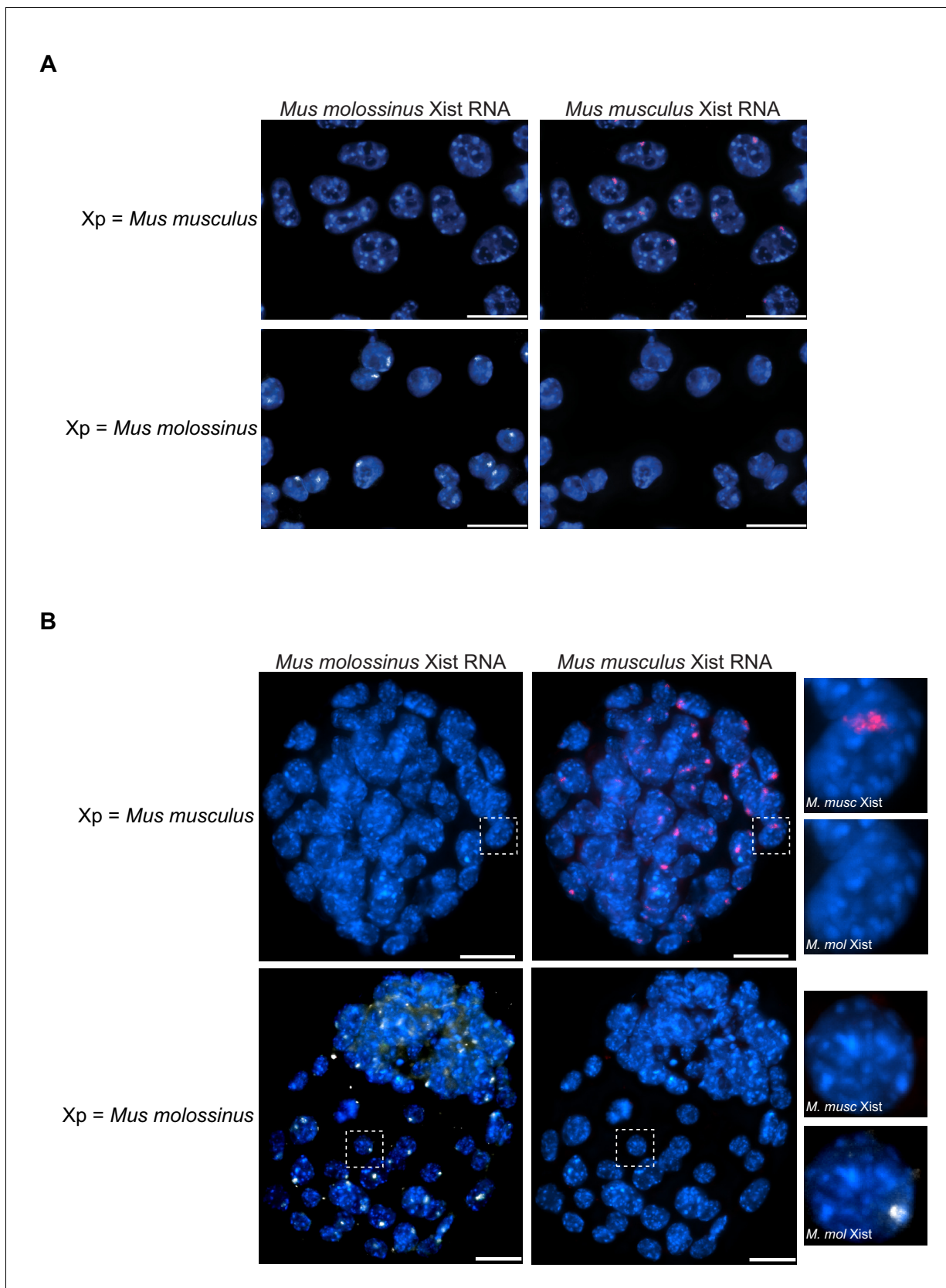


**Figure 6—figure supplement 1.** Characterization of allele-specific Xist RNA FISH probe in cells and embryos. (A) Female Trophoblast stem (TS) cells (top panel) and extraembryonic endoderm (XEN) stem cells (bottom panel) stained with an allele-specific Xist RNA FISH probe. Both TS cells and XEN

Figure 6—figure supplement 1 continued on next page



## Figure 6—figure supplement 1 continued

cells express Xist from and undergo imprinted X-inactivation of the paternal X-chromosome (Kunath et al., 2005; Tanaka et al., 1998). The TS cells are derived from a cross of JF1 *Mus molossinus* dam with a 129/S1-derived *Mus musculus* sire. The XEN cells are generated from a cross of 129/S1 *Mus musculus* dam and JF1 *Mus molossinus*-derived sire. In the TS cells, the paternal-X is therefore *Mus musculus* derived while in the XEN cells the paternal-X is JF1 *Mus molossinus* derived. *Mus musculus*-specific Xist RNA FISH probe detects the complimentary Xist RNA in red and the *Mus molossinus*-specific Xist RNA FISH probe detects its complimentary Xist RNA in white. (B) *Eed*<sup>fl/+</sup> female E3.5 embryos stained with the same allele-specific Xist RNA FISH probe as in (A). Top panels, representative stained embryo derived from a cross of *Eed*<sup>fl/fl</sup>;X<sup>JF1</sup>X<sup>JF1</sup> *Mus molossinus*-derived dam with a *Mus musculus* sire. Bottom panels, representative stained embryo from an *Eed*<sup>fl/fl</sup> *Mus musculus*-derived dam with a JF1 *Mus molossinus*-derived sire (this embryo is also shown in Figure 6A). Due to imprinted X-inactivation, both E3.5 embryos are expected to express Xist RNA from their paternal X-chromosome.

DOI: <https://doi.org/10.7554/eLife.44258.014>



**Figure 7.** Switching of imprinted to random X-inactivation in 3–16 cell embryos lacking maternal EED. (A,B) Allele-Specific Xist RNA FISH in *Eed*<sup>fl/+</sup> and *Eed*<sup>m-/-</sup> female and male 3–16 cell embryos. Xist RNA expressed from the maternal X-chromosome is indicated in red and from the paternal X-chromosome in white. Representative embryos are depicted. Nuclei are stained blue with DAPI. Scale bars, 20  $\mu$ m.

DOI: <https://doi.org/10.7554/eLife.44258.015>

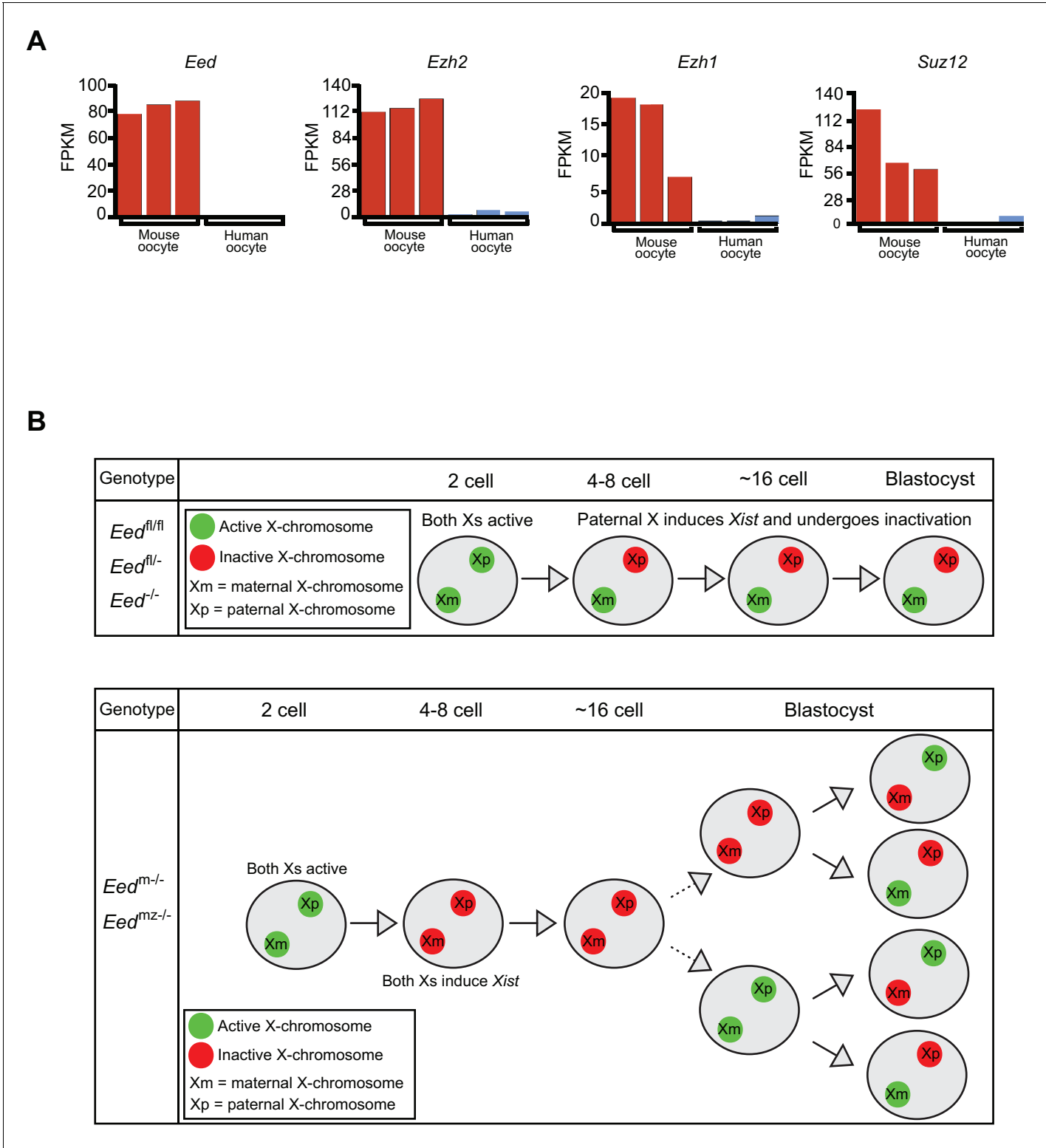


**Figure 8.** Lack of PRC2 expression in human oocytes and a path to randomization of X-inactivation in early embryos. (A) Expression levels by RNA-Seq of core PRC2 components in human and mouse oocytes. (B) Model of maternal PRC2 function during preimplantation mouse embryogenesis.

DOI: <https://doi.org/10.7554/eLife.44258.016>